The Astrophysical Journal, 828:48 (10pp), 2016 September 1 doi:10.3847/0004-637X/828/1/48

CLUSTER DYNAMICS LARGELY SHAPES PROTOPLANETARY DISK SIZES

Kirsten Vincke and Susanne Pfalzner
Max Planck Institute for Radio Astronomy, Auf dem Hügel 69, D-53121 Bonn, Germany; kvincke@mpifr-bonn.mpg.de
Received 2015 November 23; revised 2016 June 20; accepted 2016 June 21; published 2016 August 29

ABSTRACT

To what degree the cluster environment influences the sizes of protoplanetary disks surrounding young stars is still an open question. This is particularly true for the short-lived clusters typical for the solar neighborhood, in which the stellar density and therefore the influence of the cluster environment change considerably over the first 10 Myr. In previous studies, the effect of the gas on the cluster dynamics has often been neglected; this is remedied here. Using the code NBody6++, we study the stellar dynamics in different developmental phases—embedded, expulsion, and expansion—including the gas, and quantify the effect of fly-bys on the disk size. We concentrate on massive clusters ($M_{\rm cl} \geqslant 10^3$–$6 * 10^4\ M_{\rm Sun}$), which are representative for clusters like the Orion Nebula Cluster (ONC) or NGC 6611. We find that not only the stellar density but also the duration of the embedded phase matters. The densest clusters react fastest to the gas expulsion and drop quickly in density, here 98% of relevant encounters happen before gas expulsion. By contrast, disks in sparser clusters are initially less affected, but because these clusters expand more slowly, 13% of disks are truncated after gas expulsion. For ONC-like clusters, we find that disks larger than 500 au are usually affected by the environment, which corresponds to the observation that 200 au-sized disks are common. For NGC 6611-like clusters, disk sizes are cut-down on average to roughly 100 au. A testable hypothesis would be that the disks in the center of NGC 6611 should be on average ≈20 au and therefore considerably smaller than those in the ONC.

Key words: galaxies: star clusters: general – planetary systems – protoplanetary disks

1. INTRODUCTION

Most stars are born in stellar clusters, which in turn form from dense cores in giant molecular clouds (GMCs). At least for massive clusters ($M_{\rm cl} > 10^3\ M_{\odot}$), it is known that they are highly dynamical structures and follow well-defined evolutionary tracks, depending on their initial mass and size (Pfalzner & Kaczmarek 2013b). At very young ages, they are still embedded in their natal gas; the duration of this embedded phase is thought to last between 1 and 3 Myr for clusters in the solar neighborhood (Leisawitz et al. 1989; Lada & Lada 2003; Portegies Zwart et al. 2010). Comparing the gas and stellar content in nearby star forming regions, observations find that the fraction of gas in a GMC that is turned into stars (referred to as star formation efficiency—SFE) lies in the range of 10%–35% (Lada & Lada 2003). Similarly, simulations that model the expansion history of massive clusters in the solar neighborhood find that the SFE of these clusters must have been of the order of 30% (Pfalzner & Kaczmarek 2013b). In comparison, the SFE for an entire molecular cloud is much lower, only of the order of just a few percent at most (see, e.g., Murray 2011; García et al. 2014).

At the end of the star formation process, the remaining gas is expelled through various mechanisms such as, for example, the explosion of a supernova (Zwicky 1953; Pelupessy & Portegies Zwart 2012), bipolar stellar outflows (Matzner & McKee 2000), or stellar winds of the most massive stars (Zwicky 1953; Dale et al. 2012; Pelupessy & Portegies Zwart 2012; Dale et al. 2015). It is expected that supernovae will ultimately remove any remaining gas from the cluster, but probably other processes like wind are more important, as clusters are already found to be gas poor at 1–3 Myr, whereas even supernova with 25 $M_{\rm Sun}$ need already 7–8 Myr until they explode. The gas expulsion itself is thought to happen on timescales smaller than, or of the order of, the dynamical times of the cluster (Geyer & Burkert 2001; Melioli & de Gouveia dal Pino 2006; Portegies Zwart et al. 2010). Gas expulsion is supposed to happen earlier in massive than in low-mass clusters due to the larger number of high-mass stars.

The gas expulsion leaves the clusters in a supervirial state and they react by expanding with a simultaneous loss of a considerable portion of their members. The cluster dynamics after gas expulsion has been investigated thoroughly in the past (e.g., Lada et al. 1984; Goodwin 1997; Adams 2000; Geyer & Burkert 2001; Kroupa et al. 2001; Boily & Kroupa 2003a, 2003b; Fellhauer & Kroupa 2005; Goodwin & Bastian 2006; Baumgardt & Kroupa 2007; Lüghausen et al. 2012; Pfalzner et al. 2014, 2015b).

Within the clusters, their members interact with each other, influencing already formed protoplanetary disks. Processes like external photoevaporation (Johnstone et al. 1998, 2004; Störzer & Hollenbach 1999; Scally & Clarke 2002; Matsuyama et al. 2003; Adams et al. 2006; Alexander et al. 2006; Ercolano et al. 2008; Drake et al. 2009; Gorti & Hollenbach 2009), viscous torques (Shu et al. 1987), turbulent effects (Klahr & Bodenheimer 2003), and magnetic fields (Balbus & Hawley 2002) are capable of reducing the disks in size, mass, and/or angular momentum.

However, here we concentrate on the effect of the gravitational forces acting during close stellar fly-bys, which shape the disks, resulting in the loss of angular momentum (e.g., Pfalzner & Olczak 2007) and/or mass (e.g., Clarke & Pringle 1993; Hall 1997; Scally & Clarke 2001; de Juan Ovelar et al. 2012).

Ideally, one would simulate the entire cluster with each of the stars surrounded by a disk using the smoothed particle hydrodynamics (SPH) methods. In this case, effects like viscous spreading of the disks and multiple fly-bys would all be treated in a self-consistent way. Still, even with modern supercomputers, this is extremely challenging. Rosotti et al. (2014) performed a direct theoretical investigation of disk sizes

in clusters by combining *N*-body simulations of a low-mass cluster (100 stars) with SPH simulations of protoplanetary disks and determined the disk sizes. Even for such a low-mass cluster, they could only model the first 0.5 Myr of the development and had to make the artificial assumption of the stars to be of equal mass due to computational constraints. Thus, for the time being, direct modeling of massive clusters, and even more so a parameter study of them, is completely out of the question.

Therefore, the standard procedure is a two step approach. - First, *N*-body simulations of the cluster dynamics are performed where the fly-by history of each star is recorded and, second, results from parameter studies are used to post-process the data and determine the effect on the disks (e.g., Scally & Clarke 2001; Olczak et al. 2006; Pfalzner et al. 2006; Olczak et al. 2010; Steinhausen & Pfalzner 2014). These studies concentrated on the disk frequency, average disk mass, and angular momentum in the embedded phase of the cluster. However, none of these studies considered the gas content as such or the effect that the gas expulsion process has on the cluster dynamics. Here we want to concentrate instead on the disk size, because (a) it is the most sensitive indicator for the cluster influence (Rosotti et al. 2014; Vincke et al. 2015), (b) with the advent of ALMA, a direct comparison with observations is possible, and (c) it gives limits on the sizes of the potentially forming planetary systems that can be compared to exoplanetary systems.

There have been a few studies that investigated the influence of fly-bys on the disk size. However, they were usually based on the results from parameter studies of fly-bys between equal-mass stars (Clarke & Pringle 1993; Kobayashi & Ida 2001; Adams 2010). A real cluster contains a wide spectrum of masses and therefore equal-mass fly-bys are the exception rather than the rule (Pfalzner & Olczak 2007). Others proposed to convert the disk-mass criterion of Olczak et al. (2006) directly into a disk size (de Juan Ovelar et al. 2012). Nevertheless, Breslau et al. (2014) showed that this approach is error prone and devised a relation for the disk size after an fly-by that is valid over a large range of mass ratios between the star and the perturber.

Vincke et al. (2015), in the following referred to as VBP15, used this more appropriate description of the effect of fly-bys on the disk size to perform a study on embedded clusters of different mass and stellar density. They found that fly-bys in the embedded phase are capable of reducing disks to sizes well below 1000 au and that the median disk size strongly depends on the stellar density. However, as in all previous studies, they did not take into account the presence of the gas in the embedded phase and the effect of gas expulsion on the cluster dynamics.

In contrast to previous studies, we include here the effect of the gas on the cluster dynamics and model all the evolutionary stages of the clusters self-consistently—the embedded phase, the gas expulsion, and the expansion phase. We quantify the differences between the fly-by history in the embedded phase and the expansion phase. More importantly, we will demonstrate how the differences in cluster dynamics and timescales influence the fly-by dynamics and the final disk-size distribution in dense and sparse clusters.

2. METHOD

2.1. Cluster Simulations

The cluster simulations are performed using the code Nbody6++ (Aarseth 1973; Spurzem 1999; Aarseth 2003). We model clusters of different mass, which is realized by performing simulations of clusters with different numbers of stars: 1000 (E0), 2000 (E1), 4000 (E2), 8000 (E3), 16,000 (E4), and 32,000 (E52, E51). However, the initial size of the clusters is kept fixed at a half-mass radius of $r_{\rm hm} = 1.3$ pc, which allows us to study clusters of different density. Clusters depicted, e.g., in Lada & Lada (2003) usually have somewhat smaller radii (<1 pc) as they still form stars. There are strong indications that clusters' sizes increase with age during the star formation process and are typically about 1–2 pc by the time star formation is finished (Kroupa 2005; Pfalzner & Kaczmarek 2013a; Pfalzner et al. 2014).

Currently, it is not clear to what extent massive clusters are subject to substructure. Any potentially existing substructure is quickly erased in the star formation phase (Bonnell et al. 2003; Parker et al. 2014), at the latest the gas expulsion will eliminate any left-over substructure in the presented extended clusters. For simplicity, we assume here an initial stellar number density distribution according to a relaxed, smooth King distribution (Olczak et al. 2010) with a flat core, which is representative for the Orion Nebula Cluster (ONC), which is at the onset of gas expulsion and one of the best studied massive clusters in the solar neighborhood. A detailed description of the density distribution, including an illustration of the initial density distribution as a function of the cluster radius (their Figure 1), can be found in Olczak et al. (2010). Any potentially existing substructure would make close encounters more common, so that the results presented here can be regarded as lower limits for the importance of the cluster environment on the protoplanetary disks. In contrast to VBP15 and most previous work, here we take into account the potential of the gas component as well. The total mass of the system $M_{\rm cl}$ is $M_{\rm cl} = M_{\rm stars} + M_{\rm gas}$ with $M_{\rm stars}$ being the stellar component of the cluster; therefore, the gas mass is given by

$$M_{\rm gas} = \frac{M_{\rm stars}(1 - {\rm SFE})}{\rm SFE}. \quad (1)$$

where SFE is the star formation efficiency, which is assumed to be 30%. Various studies have shown that such SFEs are characteristic for massive clusters like NGC 2244, NGC 6611 etc. in the solar neighborhood (for example, Lada & Lada 2003). The stars are initially still embedded in the remaining gas. Note that the gas density profile was chosen to be of the Plummer form (Steinhausen 2013) with a half-mass radius similar to that of the stellar profile (1.3 pc), because King gas profiles lead to numerical difficulties.

Apart from Rosotti et al. (2014), all previous studies of this kind did not include the gas component, including it here basically results in a different velocity dispersion compared to the gas-free case. It is assumed that the cluster is initially in virial equilibrium. The stellar velocities and the individual stellar masses are sampled randomly, the former from a Maxwellian distribution, the latter from the IMF by Kroupa (2002) with a lower stellar mass limit of 0.08 $M_\odot$ and an upper mass limit of 150 $M_\odot$. The embedded phase of clusters is thought to last between 1 and 3 Myr (Leisawitz et al. 1989; Lada & Lada 2003; Portegies Zwart et al. 2010). Accordingly,

Table 1
Cluster Model Setup and Dynamical Timescales

Model	N_{stars}	N_{sim}	t_{emb} (Myr)	r_{hm} (pc)	M_{stars} ($M_\odot$)	M_{cl} ($M_\odot$)	t_{dyn} (Myr)
E0	1000	308	2.0	1.3	590.8	1969.2	0.67
E1	2000	168	2.0	1.3	1192.2	3973.9	0.47
E2	4000	94	2.0	1.3	2358.1	7860.3	0.33
E3	8000	47	2.0	1.3	4731.2	15770.6	0.24
E4	16000	16	2.0	1.3	9464.8	31549.3	0.17
E52	32000	9	2.0	1.3	18852.6	62842.0	0.12
E51	32000	7	1.0	1.3	18839.2	62797.3	0.12

Note. Column 1 indicates the model designation, followed by the initial number of stars in the cluster N_{stars}, the number of simulations in campaign N_{sim}, the duration of the embedded phase t_{emb}, the initial half-mass radius r_{hm} of the cluster, the stellar mass of the cluster M_{stars}, the total cluster mass (including the gas mass) M_{cl}, and the resulting dynamical timescale t_{dyn}. For calculation of M_{cl} and t_{dyn}, see the text.

we simulated clusters with an embedded phase lasting $t_{emb} = 2$ Myr, but also performed an additional set of simulations for the densest cluster with $t_{emb} = 1$ Myr (model E51). This allows us to also study how the length of the embedded phase influences the final distribution of protoplanetary disk sizes. For a more detailed summary of the set-up parameters, see Table 1.

In contrast to previous work, we take into account that the gas expulsion process typically happens after 1–3 Myr. The gas expulsion itself happens on short timescales, typically smaller than, or of the order of, several dynamical times t_{dyn} of the cluster (Geyer & Burkert 2001; Melioli & de Gouveia dal Pino 2006; Portegies Zwart et al. 2010), which is given by

$$t_{dyn} = \left(\frac{GM_{cl}}{r_{hm}^3}\right)^{-1/2}. \quad (2)$$

The dynamical timescales for the cluster models E0-E52 are very short, between 0.8 and 0.14 Myr, see column 7 of Table 1. Therefore, and for better comparability of our cluster models, we assume the gas expulsion process in all clusters to be instantaneous. This immediate removal of the gas mass after $t = t_{emb}$ leaves the cluster in a supervirial state, so that the cluster expands in order to regain virial equilibrium. We will discuss the consequences of such an instantaneous gas expulsion on the results compared to a longer expulsion timescale in Section 4. We follow the cluster expansion until 10 Myr have passed since the cluster was fully formed.

In each simulation, the fly-by history for each individual star was tracked and the fly-by properties recorded. For each cluster model, a campaign of simulations with different random seeds was performed in order to improve statistics and minimize the effect of the initial individual setup of a cluster on the results. The number of simulations for each setup is given in column 3 of Table 1.

2.2. Disk Size Development

Ideally, one would start out the simulation with an observed primordial disk size. However, observationally it is challenging to measure disk sizes directly especially in embedded clusters. In contrast to the disk fraction, disk size measurements are usually performed in (nearly) exposed clusters, which have expelled most of their gas. For the best observed stellar cluster in the solar neighborhood, the ONC, disk radii in the range from ~27 au up to ~500 au were found by several surveys (McCaughrean & O'dell 1996; Vicente & Alves 2005; Eisner et al. 2008; Bally et al. 2015). However, the ONC is already 1 Myr old. Whether these measurements are representative for the primordial disk-size distribution or whether photoevaporation or fly-by processes have already altered the sizes remains unclear. In other clusters, disk sizes up to several thousand astronomical units have been reported. Therefore, there is no information about a typical initial disk size or a disk-size distribution in embedded stellar clusters.

For this reason, and for simplicity, all disks in a cluster are set up with the same initial size r_{init}, ignoring any possible dependency of the disk size on the host mass (see Hillenbrand et al. 1998; Vicente & Alves 2005; Eisner et al. 2008; Vorobyov 2011; Vincke et al. 2015). We performed a numerical experiment, setting the initial disk size to a very large value of $r_{init} = 10{,}000$ au. The interpretation of this large initial disk size will be discussed in Sections 3 and 4.

In our simulations, we determine the size of the protoplanetary disks around the cluster members after each stellar fly-by using the equation

$$r_{disc} = \begin{cases} 0.28 \cdot r_{peri} \cdot m_{12}^{-0.32}, & \text{if } r_{disc} < r_{previous} \\ r_{previous}, & \text{if } r_{disc} \geqslant r_{previous}, \end{cases} \quad (3)$$

given by Breslau et al. (2014), where $m_{12} = m_2/m_1$ is the mass ratio between the disk-hosting star (m_1) and the perturber (m_2), r_{peri} is the periastron distance in astronomical units, and $r_{previous}$ is the disk size previous to the fly-by in astronomical units. This equation is valid for coplanar, prograde, parabolic fly-bys. This type of fly-by is more destructive than inclined, retrograde, or hyperbolic fly-bys (Clarke & Pringle 1993; Heller 1995; Hall 1997; Pfalzner et al. 2005c; A. Bhandare & S. Pfalzner 2016, in preparation). However, the effect of inclined, retrograde and hyperbolic fly-bys is much less investigated. First results by Bhandare & Pfalzner indicate that non-coplanar encounters have, nevertheless, a considerable effect on the disk size. Thus, the here presented result has to be regarded as the lower limit of disk size, but will not be considerably smaller than it would be in the inclined case.

Viscous forces, which might lead to disk spreading (Rosotti et al. 2014), and self-gravity between the disk particles are neglected in this model because the disks are set up containing only massless tracer particles. Every star in the cluster was surrounded by such a massless disk; therefore, each fly-by event is actually a disk–disk fly-by. Capturing of material from the disk of the passing star is disregarded in our approach as well. The formula above only holds for star–disk fly-bys, where only the primary hosts a disk. Nevertheless, Pfalzner et al. (2005a) found that a generalization of disk–disk fly-bys to star–disk fly-bys is valid as long as the disks have a low mass and not much mass is transferred between the two. For a more detailed description of the disk-size determination, its approximations, and the resulting influence on the results, see, Breslau et al. (2014). At the end of the diagnostic step the resulting fly-by and disk-size statistics are averaged over all simulations within one simulation campaign.

Before presenting the results, we want to elucidate some definitions used in the following section. We use the term "fly-by" in our study for gravitational interactions between two stars

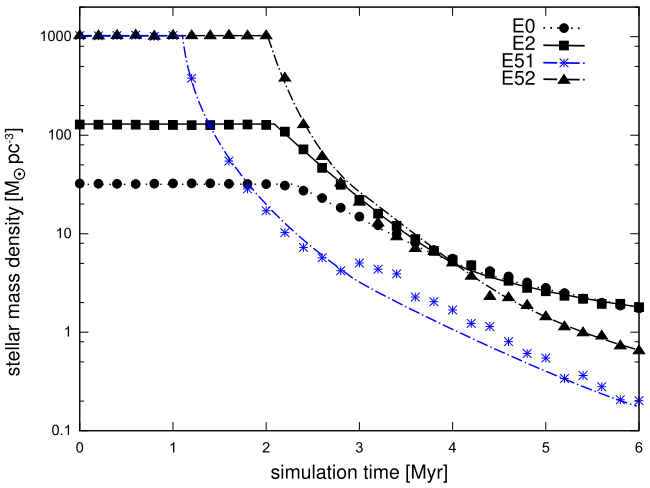

Figure 1. Stellar mass density within 1.3 pc (initial half-mass radius) as a function of time for clusters of different densities: E0 (dots), E2 (squares), E51 (asterisks, blue), and E52 (triangles). The duration of the embedded phase is $t_{\rm emb} = 1$ Myr for E51 and $t_{\rm emb} = 2$ Myr for all other models.

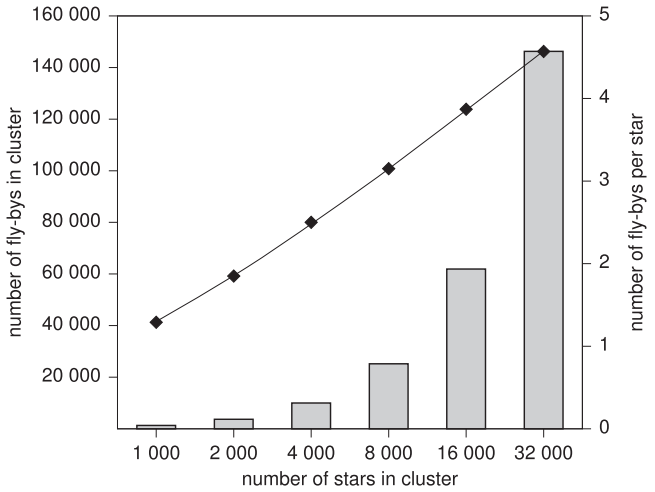

Figure 2. Number of fly-bys per cluster (gray boxes, left y-axis) and per star (black diamonds, right y-axis) for the different cluster models. The black line only serves to guide the eye.

that (a) reduce the disk size by at least 5% ($r_{\rm disk}/r_{\rm previous} \leqslant 0.95$). The term "strongest fly-by" or "disk-size defining fly-by" describes the fly-by with the strongest influence on the disk in the whole simulation—or for certain periods of cluster evolution. Note that, as Equation (3) takes into account the mass ratio of the perturber and the host star, the strongest fly-by is not necessarily the closest one.

3. RESULTS

The cluster evolution, namely the same mass and radius development—confirm previous work. However, here we have a closer look at the density evolution because this determines the fly-by history investigated here. Our simulations show that, as long as the clusters remain embedded in their natal gas ($t_{\rm emb} = 2$ Myr, for model E51 $t_{\rm emb} = 1$ Myr), the stellar mass density basically stays constant (see Figure 1). When the gas is expelled instantaneously at $t = t_{\rm emb}$, the clusters respond to the now supervirial state by expanding, leading to a significant drop in the stellar density.

The more massive clusters regain their virial equilibrium much faster than the less massive clusters (Parmentier & Baumgardt 2012; Pfalzner & Kaczmarek 2013a) due to their shorter dynamical timescales, see Table 1. As a result, their stellar density declines faster than in the lower mass clusters—the density in the most massive cluster (triangles and asterisks) drops to 10% of its initial value already $t = 0.3$ Myr after gas expulsion, whereas low-mass clusters need up to $t = 2$ Myr after gas expulsion for such a decline.

Note that around $t = 3$–4 Myr, the cluster models E0, E2, and E52 are indistinguishable in terms of their stellar mass density within 1.3 pc, while having a very different density history.

Naturally, the total number of fly-bys increases with cluster density, which in our case is equivalent to the cluster mass. In the least dense cluster roughly 1300 fly-bys that change the disk size take place during the 10 Myr simulated here whereas in the densest cluster model the number of fly-bys is approximately 150,000 (see Figure 2). However, this increase is by far not as much as one would expect from a roughly 32 times higher density of models E51 and E52 in the embedded phase (see Figure 1). The reason is that we only consider fly-bys that lead to a smaller disk size than previous to the fly-by, see Section 2. For the dense clusters the disk sizes are reduced very quickly to very small sizes so that even closer disk-size changing fly-bys are rare at later times. Similarly, the number of fly-bys per star increases with cluster density. In model E0, each star undergoes, on average, a little more than one disk-size changing fly-by as defined above, whereas in model E52 its between four and five. Although the difference in density (within the half-mass radius) between these two models is almost a factor of 100, the average number of fly-bys increases almost linearly by a factor of four due to the criteria mentioned above.

This is also reflected in the temporal development of the number of disk-size changing fly-bys. Figure 3 (a) depicts the fly-by history in the different cluster models. It shows the cumulative fraction of fly-bys as a function of time, where the vertical lines mark the time of gas expulsion (1 Myr for model E51, dotted blue, 2 Myr all other models, solid black). The steeper slopes for the most massive clusters indicate that the disks are processed faster. For example, more than 50% of all disk-size reducing fly-bys in model E52 occur within the first 0.2 Myr, whereas in model E0 it takes four times as long (~0.8 Myr) for the same portion of fly-bys to happen.

As to be expected, the majority of fly-bys happens in the dense embedded phase. However, there are differences between the different cluster types, see Figure 3 (b). Whereas in the most massive clusters disk-size changes happen nearly exclusively (~98%) in the embedded phase (black)—and most even within the first few 100,000 years—in the least dense clusters, only 87% of all disk-size changes occur in this phase. The reason for this is that, in the latter case, the density decreases more slowly so that a higher fraction of about one-seventh of disk-size reducing fly-bys happens in the expansion phase (gray).

Obviously, the length of the embedded phase plays an important role. In model E51, the gas is expelled after 1 Myr, whereas for model E52 the gas expulsion happens after 2 Myr. The earlier drop in cluster mass density in model E51 results in the total number of fly-bys in model E52 being roughly 15% larger than in model E51 (151,000 compared to 131,000).

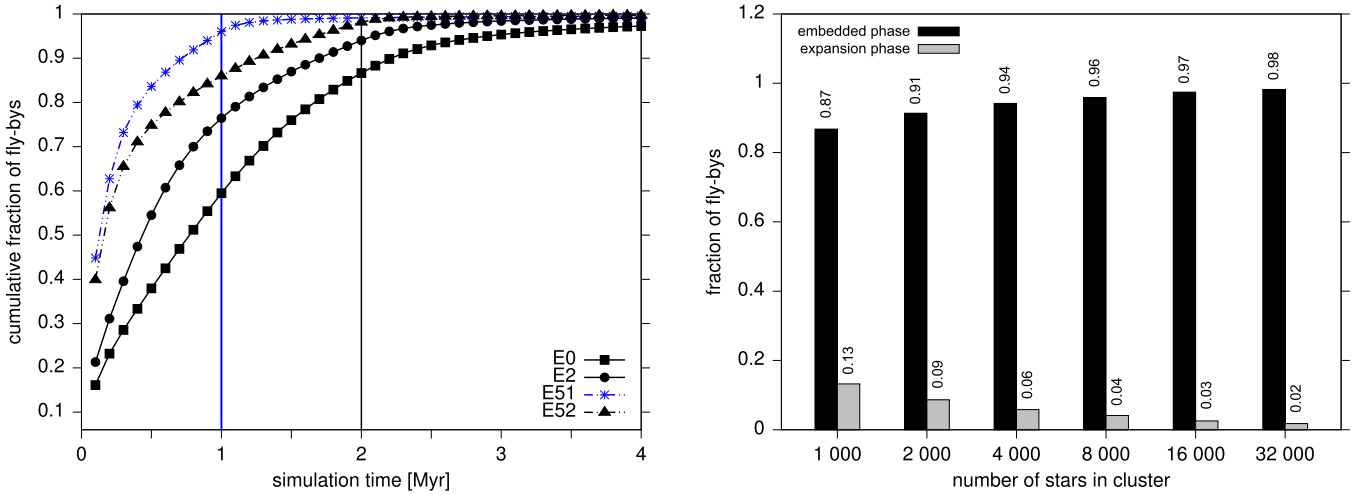

Figure 3. (Left) Cumulative fraction of fly-bys as a function of time for the cluster models E0 (squares), E2 (dots), E51 (asterisks, blue), and E52 (triangles). The vertical lines depict the points in time of gas expulsion for model E51 (1 Myr, dotted blue) and for all other models (2 Myr, solid black). (Right) Fraction of fly-bys as a function of the number of stars in the cluster for the embedded phase (black) and the expansion phase (gray).

Again, the reason why the number of fly-bys does not double for a twice as long embedded phase is that most of the disks have been reduced to a small disk size during the first million years and therefore the cross-section for a disk-size changing fly-by has been reduced. This means that the early embedded phases largely determine the disk sizes.

The distinct clusters have very different influences on their protoplanetary disks, reflected, for example, in the overall median disk size (Figure 4). This median disk size is about 13 times smaller in model E52 (32,000 stars) than in model E0 (1000 stars) because not only does the number of fly-bys increase significantly with cluster density, but the fly-bys are on average also closer or the mass ratio is higher. For the densest clusters, most fly-bys happen at the beginning of the embedded phase, thus, the median disk sizes are nearly the same at the end of the embedded phase (∼108 au, open squares) and at the end of the simulations (∼104 au, dots). However, for model E0, the median disk size is significantly larger (∼1670 au) at the end of the embedded phase (2 Myr) than at the end of the simulations (∼1350 au) as roughly one-seventh of the close fly-bys occur in the expansion phase.

It is important to note that we do not expect real disks to be generally as large as nearly 1700 au. The median disk size here only reflects the degree of the environment's influence on the disks. For example, as long as the disks are initially >100 au, they are reduced in size in the densest cluster model. By contrast, in the ONC model only disks that are initially larger than ∼500 au are affected. A real initial disk size distribution would be necessary to further constrain this, for a more detailed discussion, see Section 4.

What does the spatial disk size distribution at the end of embedded phase look like? Figure 5 (a) shows the median disk size as a function of the distance to the cluster center of the stars for different cluster models at $t = 2$ Myr (open black symbols). In the inner part of the ONC-like cluster (E2), for example, within a sphere of the initial half-mass radius (1.3 pc) the median disk sizes are considerably smaller than for the clusters outskirts. The difference is even larger when one compares the extremes—the median disk size rises from 50 au at 0.1 pc to 2000 au at 4 pc. This is due to the higher density in the cluster core and the resulting higher fly-by frequency.

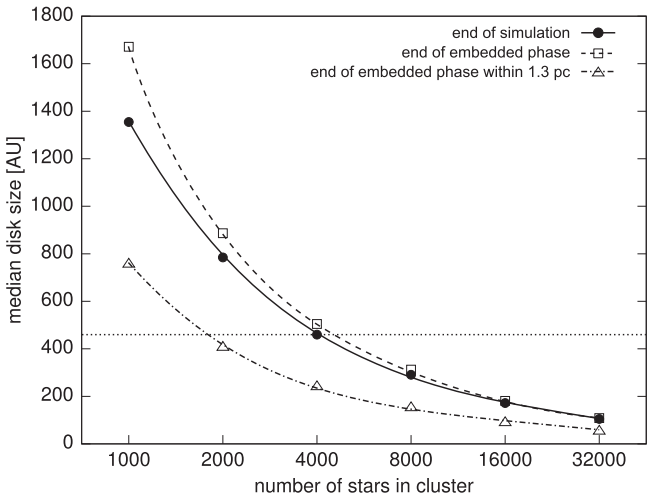

Figure 4. Overall median disk size for all stars for different cluster models at the end of the simulation (10 Myr, dots), at the end of the embedded phase (2 Myr, squares), and at the end of the embedded phase within a sphere of 1.3 pc (initial half-mass radius, triangles).

These trends have already been seen in simulations where the gas content was neglected (VBP15), however, there are quantitative differences. Figure 5(b) compares the median disk size as a function of the distance to the cluster center after 2 Myr of simulation time for the ONC cluster model (E2) obtained in VBP15 (open squares) and in this work (circles). Including the gas mass explicitly leads to a higher velocity dispersion in the embedded phase and thus stronger encounters. Therefore, the median disk sizes presented in this work are much smaller than in VBP15. For example, at the rim of the cluster core (0.3 pc), the median disk size in the work here is more than a factor of four smaller than in VBP15 (∼108 au compared to ∼470 au). At a distance of 1 pc, the situation is even more extreme, as in our work, the median disk size is roughly 400 au, whereas in VBP15 more than half of the disks are not influenced at all and still retain their initial size.

If we consider the first 10 Myr of cluster evolution, which includes the embedded, gas expulsion, and expansion phases

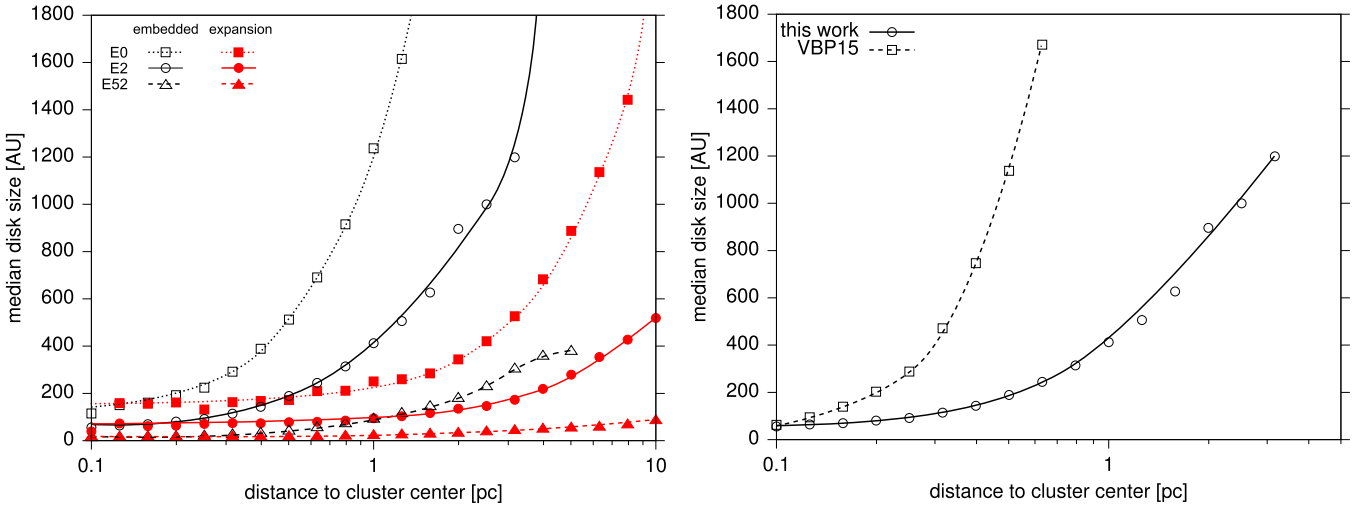

Figure 5. Median disk size as a function of the distance to the cluster center (left panel) for different cluster models (E0 squares, E2 circles, and E52 triangles) at the end of the embedded phase (2 Myr, black symbols) and at the end of the simulation covering the embedded, the gas expulsion, and the expansion phases (10 Myr (red symbols); (right panel) for the ONC model (E2) in this work, i.e., with gas mass (circles, same as in (a)), and in VBP15, i.e., without gas mass (squares). The lines in both panels only serve to guide the eye.

(black symbols in Figure 5), in general, the denser the cluster is, the smaller the median disk size remains. Nonetheless, after 10 Myr, the median disk size is nearly constant (at least for models E2 and E52) within 3 pc from the cluster center. This is not so much due to mixing, but basically mostly caused by the expansion of the cluster—the value of the median disk size in the cluster outskirts is now similar to that in the center at the end of the gas expulsion (2 Myr). While during the embedded phase most stars do not move significantly in radial directions and the dependence of the median disk size on the distance to the cluster center is preserved, after gas expulsion only about 10% of stars remain bound to the cluster and the rest leaves the cluster very quickly (Fall et al. 2009; Dukes & Krumholz 2012). The still bound stars largely move to positions more distant from the cluster center than they were originally. That is the reason why the median disk size throughout the cluster in the expansion phase is similar to the median disk size in the inner cluster region shortly before gas expulsion. This means that when older clusters are observed they work like a microscope showing us the central area of enlarged versions of younger clusters.

If observations of older clusters work like a microscope, what would an observed disk-size distribution in a cluster at different ages look like? To answer this question, we investigate the ONC-model cluster (E2) at different ages with an artificial fixed field of view (FOV) ($r_{\rm FOV} = 1$ pc) to mimic observations. Note that the FOVs for observations are usually squares, whereas here we present spheres with radii of $r_{\rm FOV}$, centered on the cluster origin. Figure 6 shows the resulting disk-size statistics for an ONC-like cluster at 1 Myr (white), 2 Myr (gray), and 10 Myr (black). The total number of small disks increases much stronger than the number of disks with sizes of several hundreds of astronomical units. The reason for this is that, in the embedded phase, disks that are already influenced but still a few hundreds of astronomical units large still reduced in size by follow-up encounters. In comparison, the shape of the disk-size distribution barely changes between the end of the embedded phase and the end of the simulations.

Observations usually study only the central areas of a cluster, because there the stellar density of cluster members is so high

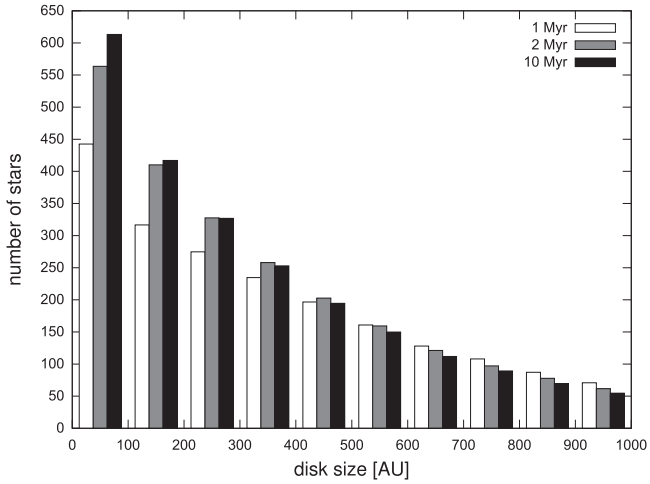

Figure 6. Disk-size distribution in the ONC-like cluster model (E2) for a fixed virtual FOV (1 pc) and different time steps: 1 Myr (white), 2 Myr (gray), and 10 Myr (black).

that member identification is relatively easy—basically, the rate of false-positives is very low. However, this concentration on the cluster center is problematic, especially for clusters after gas expulsion, which span large areas. Taking our results as a guideline, the observed median disk size in an ONC-like cluster 10 Myr after cluster formation, for example, would be ~50 au in the cluster core (0.2 pc), whereas the overall median disk size is more than nine times as large (~460 au, the dotted horizontal line in Figure 4).

Choosing initially artificially large disks of 10,000 au has the advantage that the obtained results can be applied to any smaller, real disk size. Thus, Figure 7, tells us, for example, that if all stars had an initial disk size of $r_{\rm init} \geqslant 500$ au, about half of the stars had their disks severely truncated by fly-bys to disk sizes below 500 au. An initial disk size of more than 500 au is a realistic scenario as surveys found disks in the ONC with radii of 30–500 au (McCaughrean & O'dell 1996; Vicente & Alves 2005; Eisner et al. 2008; Bally et al. 2015). Note, that at an age of approximately 1 Myr, even those might already

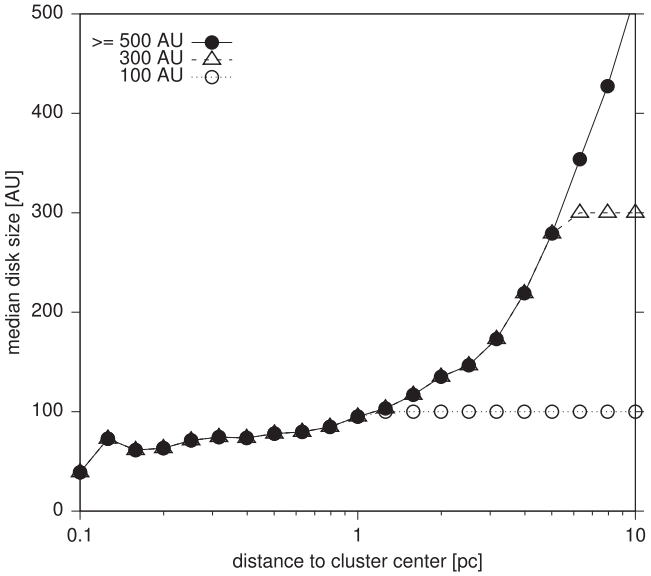

Figure 7. Median disk size at the end of the simulation (10 Myr) as a function of the distance to the cluster center for cluster model E2 for different initial disk sizes: 100 au (circles), 300 au (triangles), and ⩾500 au (dots).

have been reduced in size through photoevaporation and/or fly-bys. In the case of more massive clusters, like NGC 6611 (E52 model), there are more and closer interactions, so that independent of the initial disk size (as long as $r_{\rm init} > 100$ au) the resulting median disk is ⩽110 au, see Figure 4.

In summary, observed disk sizes or disk-size distributions in massive clusters are a strong function of the cluster age, its evolutionary stage, its initial conditions, and the FOV of the instrument. One has to act with caution when comparing and interpreting such results.

4. DISCUSSION

The above described simulations required some approximations, which we discuss in the following.

In this study, we neglect potentially existing initial substructuring of the clusters. In clusters with low velocity dispersions, the substructure will be erased quickly (see, e.g., Goodwin & Whitworth 2004; Allison et al. 2010; Parker et al. 2014). Most probably, the substructure will be erased at the end of star formation (Bonnell et al. 2003), which is when our simulations start.

The cluster models were set up without primordial mass segregation. Many clusters show signs of mass segregation, but it is unclear whether this property is primordial or if dynamical evolution caused the observed mass segregation. If we included primordial mass segregation, the most massive stars would reside in the cluster core where the density is highest. Therefore, they would undergo more fly-bys, leading in turn to smaller disks around these stars. Furthermore, stronger gravitational focussing would lead to an increase in the overall fly-by frequency in the cluster center and thus smaller disks.

All stars in the clusters were set up to be initially single excluding primordial binaries. Observations show that the multiplicity, that is, the fraction of binaries, triples, or systems of higher order, increases with stellar mass (Köhler et al. 2006; Duchêne & Kraus 2013, and references therein). The most massive stars would most probably be part of a binary then, losing their own disk quite quickly or not even forming one depending on the separation. Additionally, the gravitational focussing in the cluster due to multiple systems would be stronger than for a single, massive star, leading to an increase in the fly-by frequency and overall smaller disks.

One major difference to previous works is that we studied different evolutionary stages starting with the embedded phase, continuing with the gas expulsion, and the following expansion phase. Due to the uncertainty in the age determination of clusters, the duration of the embedded phase is not well constrained by observations. Here we modeled the duration of the embedded phase as 2 Myr. However, for the most massive clusters, this is probably too long, as at that age massive clusters are already largely devoid of gas. As most of the disk-size reducing fly-bys occur during the early stages of the embedded phase, with only 12% of fly-bys happening in the second half of the embedded phase for the most massive clusters, our results should not be very sensitive to the assumed duration of the embedded phase.

The assumption of instantaneous gas expulsion is most likely justified for the most massive clusters in our investigation (e.g., Geyer & Burkert 2001; Melioli & de Gouveia dal Pino 2006; Portegies Zwart et al. 2010). Nevertheless, for the lowest mass clusters, this is less certain. In this case, a "slow" gas expulsion lasting several million years would give the cluster more time to adjust to the gas-mass loss and fewer stars would become unbound. Furthermore, the stellar density would remain higher for a longer time span, allowing the stars to undergo more fly-bys and resulting in smaller disks than in the presented results. The influence of only the embedded phase was studied in VBP15. Comparing this to our current work, we find that the duration of the embedded phase, e.g., for the lowest density cluster[1] is strong. At the end of the embedded phase in VBP15 —lasting unrealistically 5 Myr—the mean disk size is roughly 300 au inside 0.6 pc, compared to ∼670 au) for the here adopted 2 Myr long embedded phase. If the gas was expelled slowly, a more realistic median disk size would lie between these two extremes. Further studies with an implicitly modeled gas expulsion of a few million years are necessary to constrain this rough estimate.

Here all fly-bys were assumed to be prograde, coplanar, and parabolic. Those fly-bys have a stronger effect on the disks than their retrograde, inclined counterparts (Clarke & Pringle 1993; Heller 1995; Hall 1997; Pfalzner et al. 2005c; A. Bhandare & S. Pfalzner 2016, in preparation). However, Pfalzner et al. (2005c) found that for fly-bys with inclinations of $<45°$ the final disk properties do not differ much from the prograde coplanar case. This was confirmed by A. Bhandare & S. Pfalzner (2016, in preparation), who found that even retrograde fly-bys can have a strong effect on the disk size. Disks after inclined fly-bys would be larger than the ones presented here, but at most by a factor of 1.5–1.8.

We only considered parabolic encounters; however, the typical eccentricity of a fly-by depends on the cluster density: the higher the density, the more eccentric are the fly-bys, see Figure 8. As pointed out by Pfalzner (2004), such hyperbolic fly-bys have less influence on disks than parabolic fly-bys, making the disk sizes presented here again lower limits. A detailed parameter study of hyperbolic fly-bys and their influence on the disk size would be necessary to extend our study.

[1] model D0 in VBP15, equivalent to model E0 here.

In this work, we did not include photoevaporation, which is also capable of reducing disks in size or destroying them completely (Störzer & Hollenbach 1999; Scally & Clarke 2002; Johnstone et al. 2004; Adams et al. 2006; Alexander et al. 2006; Ercolano et al. 2008; Drake et al. 2009; Gorti & Hollenbach 2009). In the embedded phase, the stars are still surrounded by the clusters natal gas, which makes the external photoevaporation ineffective. When the gas is expelled, the disks are prone to the radiation from nearby massive stars. Nevertheless, the stars move outward and may become unbound after the gas expulsion, and the stellar density decreases significantly, making it less probable for stars to be very close to their most massive companions. Only for the small fraction of stars that have a close fly-by the radiation would further reduce the disk in size making the final disks sizes smaller than presented here.

Here we study the effect on low-mass disks. In this case, viscosity and self-gravity of the disk can be neglected during the encounter as such. However, viscosity would lead to disk spreading in the long-term. Rosotti et al. (2014) performed combined Nbody/SPH simulations of low-mass clusters including viscous disks and found viscous spreading (a) counteracting the size reduction due to stellar fly-bys and (b) making the disks prone to follow-up more distant fly-bys. Recently, Xiang-Gruess (2016) compared the results of Nbody and SPH simulations of disks after stellar fly-bys, showing that viscosity can result in warped disk structures, whereas those features are not visible in massless (purely Nbody) disks. A disk-size determination in those cases would be more complicated than in the flat, massless disks used here.

We did not consider any dependence of the disk size on the host's mass (see, e.g., Hillenbrand et al. 1998; Vicente & Alves 2005; Eisner et al. 2008; Vorobyov 2011). If the initial disk size did depend on the stellar mass, the more massive stars should have started out with larger disks than the less massive stars. Vorobyov (2011) performed simulations of disks around Class 0 and Class I stars. They set a density threshold of $\Sigma < 0.1\,\mathrm{g\,cm^{-2}}$ for material belonging to the disks and found disk sizes between roughly 100 au for low-mass stars up to a little more than 1000 au for solar-like stars. If confirmed, it would mean that disks around massive stars are more prone to size changes by the environment than low-mass stars. Furthermore, this would mean that in all clusters, except model E0, more than half of the disks around solar-like stars would be influenced strongly by stellar fly-bys, see Figure 4.

Recent simulations have tried to determine the fraction of planets that become affected by the cluster environment and either move on an eccentric orbit or become unbound (Hao et al. 2013; Li & Adams 2015). However, these simulations concentrate on the initially much denser clusters that become long-lived open clusters. This type of cluster will be studied in a follow-up paper.

5. SUMMARY AND CONCLUSION

In this paper, we studied how the cluster environment changes the sizes of disks surrounding young stars. In contrast to previous work, we took the cluster development during the first 10 Myr explicitly into account. Starting with initial conditions typical for young clusters at the end of their formation phase in the solar neighborhood, we modeled the cluster dynamics from embedded throughout the expansion phase and determined the effect on the effect of gravitational interactions between the stars on the disk sizes. These types of simulations were performed for clusters of different masses and densities.

Our findings are the following.

1. It is essential to include the gas dynamics in this kind of simulation because the larger velocity dispersion leads to more encounters and significantly smaller disk sizes than in a gas-free treatment.
2. The majority of disk-size changing fly-bys always take place in the embedded phase. However, the slower expansion phase in lower mass clusters means that here still 12% of disk-size changing fly-bys happen, in comparison to just 2% for high-mass clusters.
3. For ONC-like clusters basically only disks larger than 500 au are affected by fly-bys, whereas in NGC 6611-like clusters, cutting disks below 100 au happens for 50% of stars.
4. However, in all investigated cases the disk sizes in the dense cluster centers are much more affected than the average suggests. For example, in the NGC 6611-like case the median disk size is 54 au.
5. The duration of the embedded phase influences the final median disk size, but not as strong as one would expect, because early fly-bys reduce the disk size already, leading to smaller cross-sections for later fly-bys. In the densest cluster, the median disk size after 1 Myr is already 155 au at the end of the embedded phase 108 au, which is very close to the final median disk size of 104 au.

Often disk sizes and frequencies (e.g., Haisch et al. 2001; Mamajek 2009, and references therein) of clusters of different present density are compared to obtain information about to what degree the environment influences these properties. However, clusters are highly dynamical and their current density is not necessarily representative for the past development. We showed that between 3 and 4 Myr even the most extreme cluster models of E0 and E52 have very similar cluster mass densities within a sphere of 1.3 pc[2], see Figure 1. The faster evolution of massive clusters leads to this situation where the density in massive clusters and low-mass clusters of the same age can be similar, but the clusters themselves are in very different evolutionary stages. This means that at this specific point in time and in this sphere of 1.3 pc, fly-bys are equally likely in all of these initially very different clusters. However, if we compare the median disk sizes in these "equal-density" clusters at this point in time ($t = 4$ Myr), they differ considerably. In the least dense cluster, the median disk size is roughly 480 Myr whereas it is 270 au for the densest cluster model. The reason is that the most massive clusters were once much denser than the lower mass clusters and therefore their disk sizes are reduced to a larger degree.

The different expansion of the clusters—slow for low-density and fast for high-density systems—leads to very distinct fly-by histories and, consequently, different median disk sizes and disk-size distributions. If one looks only at the embedded phase there seems to be a direct relation between stellar density and the disk size: the higher the density, the smaller the median size. Thus it seems that this is easily testable against observations. However, taking into account the

[2] Note that the given simulation time is not synonymous with cluster age because the star formation phase is not covered by our simulations.

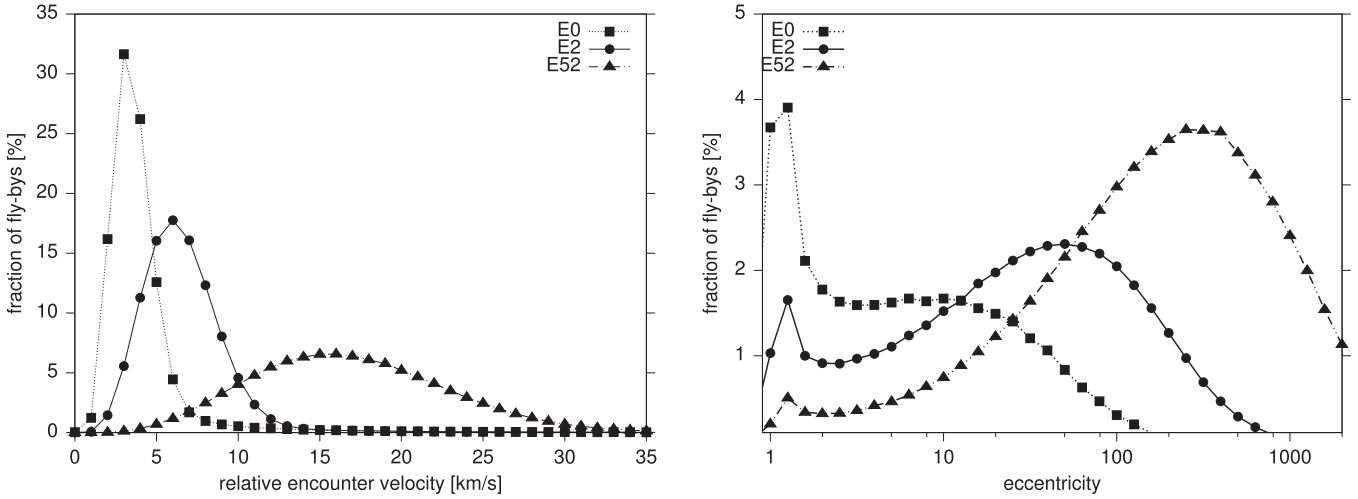

Figure 8. (Left) Relative encounter velocity distribution—that is the perturber's velocity relative the the host's velocity at the point of periastron passage—of all fly-bys and (right) eccentricity distribution of fly-bys leading to a disk size < 500 au as fractions of the total number of fly-bys for three cluster models: E0 (squares), E2 (dots), and E52 (triangles).

different evolutionary phases and their different timescales for dense and less dense clusters show that a comparison is much more complex.

All of these effects of cluster properties and observational constraints make it quite challenging to compare disk-size distributions in different clusters with each other. It does not make sense comparing the properties in clusters of different densities as long as one does not take into account their evolutionary stage and their history.

APPENDIX
FLY-BY VELOCITY AND ECCENTRICITY

The characteristics of stellar encounters change significantly with cluster density. For example, the relative velocity between two encountering stars increases for denser clusters. Figure 8(a) depicts the average relative encounter velocity—that is the velocity of the perturber relative to the host star at the time of periastron passage—for three cluster models E0 (squares), E2 (dots), and E52 (triangles). This encounter velocity can be directly correlated to the eccentricity of the perturber's orbit via

$$v_{\rm enc} = \sqrt{(1+e)\cdot\frac{G\,(m_1+m_2)}{r_{\rm peri}}}, \qquad (4)$$

where G is the gravitational constant, m_1 is the mass of the host star, m_2 is the mass of the perturber, and $r_{\rm peri}$ is the periastron distance, all in SI units. The eccentricity distribution for cluster models E0, E2, and E52 are shown in Figure 8(b) for fly-bys leading to disks smaller than 500 au.

In this study, we assumed all fly-bys to be parabolic. This approximation only holds for the least dense cluster model, as the encounter velocities and therefore the eccentricities clearly increase with cluster density (see also Olczak et al. 2010). For the denser cluster models (especially E52), a detailed study of the influence of hyperbolic fly-bys on disk sizes would be favorable. Previous studies suggest that their influence on the disks (in these cases, the disk mass and angular momentum) is much smaller than the one of parabolic encounters (for detailed discussions, see, e.g., Pfalzner et al. 2005c; Olczak et al. 2010, 2012). Therefore, the disk sizes presented here might be lower limits.

At very high densities, that is, especially in cluster model E52, fly-bys are no longer two-body encounters but many-body interactions. This leads to the extreme eccentricities of $e > 100$. Especially for this type of fly-by, we expect the disk-size change to be smaller than for the here assumed prograde, coplanar, parabolic case.

REFERENCES

Aarseth, S. J. 1973, VA, 15, 13
Aarseth, S. J. 2003, Gravitational N-Body Simulations (Cambridge: Cambridge Univ. Press)
Adams, F. C. 2000, ApJ, 542, 964
Adams, F. C. 2010, ARA&A, 48, 47
Adams, F. C., Proszkow, E. M., Fatuzzo, M., & Myers, P. C. 2006, ApJ, 641, 504
Alexander, R. D., Clarke, C. J., & Pringle, J. E. 2006, MNRAS, 369, 229
Allison, R. J., Goodwin, S. P., Parker, R. J., Portegies Zwart, S. F., & de Grijs 2010, MNRAS, 407, 1098
Balbus, S. A., & Hawley, J. F. 2002, ApJ, 573, 749
Bally, J., Mann, R. K., Eisner, J., et al. 2015, ApJ, 808, 69
Baumgardt, H., & Kroupa, P. 2007, MNRAS, 380, 1589
Boily, C. M., & Kroupa, P. 2003a, MNRAS, 338, 665
Boily, C. M., & Kroupa, P. 2003b, MNRAS, 338, 673
Bonnell, I. A., Bate, M. R., & Vine, S. G. 2003, MNRAS, 343, 413
Bonnell, I. A., & Davies, M. B. 1998, MNRAS, 295, 691
Breslau, A., Steinhausen, M., Vincke, K., & Pfalzner, S. 2014, A&A, 565, A130
Clarke, C. J., & Pringle, J. E. 1993, MNRAS, 261, 190
Dale, J. E., Ercolano, B., & Bonnell, I. A. 2012, MNRAS, 424, 377
Dale, J. E., Ercolano, B., & Bonnell, I. A. 2015, MNRAS, 451, 987
de Juan Ovelar, M., Kruijssen, J. M. D., Bressert, E., et al. 2012, A&A, 546, L1
Drake, J. J., Ercolano, B., Flaccomio, E., & Micela, G. 2009, ApJL, 699, L35
Duchêne, G., & Kraus, A. 2013, ARA&A, 51, 269
Dukes, D., & Krumholz, M. R. 2012, ApJ, 754, 56
Eisner, J. A., Plambeck, R. L., Carpenter, J. M., et al. 2008, ApJ, 683, 304
Ercolano, B., Drake, J. J., Raymond, J. C., & Clarke, C. C. 2008, ApJ, 688, 398
Fall, S. M., Chandar, R., & Whitmore, B. C. 2009, ApJ, 704, 453
Fellhauer, M., & Kroupa, P. 2005, ApJ, 630, 879
García, P., Bronfman, L., Nyman, L.-A., et al. 2014, ApJS, 212, 2
Geyer, M. P., & Burkert, A. 2001, MNRAS, 323, 988
Goodwin, S. P. 1997, MNRAS, 284, 785
Goodwin, S. P., & Bastian, N. 2006, MNRAS, 373, 752
Goodwin, S. P., & Whitworth, A. P. 2004, A&A, 413, 929
Gorti, U., & Hollenbach, D. 2009, ApJ, 690, 1539

Haisch, K. E., Jr., Lada, E. A., & Lada, C. J. 2001, ApJL, 553, L153
Hall, S. M. 1997, MNRAS, 287, 148
Hao, W., Kouwenhoven, M. B. N., & Spurzem, R. 2013, MNRAS, 433, 867
Heller, C. H. 1995, ApJ, 455, 252
Hillenbrand, L. A., Strom, S. E., Calvet, N., et al. 1998, AJ, 116, 1816
Huff, E. M., & Stahler, S. W. 2006, ApJ, 644, 355
Johnstone, D., Hollenbach, D., & Bally, J. 1998, ApJ, 499, 758
Johnstone, D., Matsuyama, I., McCarthy, I. G., & Font, A. S. 2004, RMxAA, 22, 38
Klahr, H. H., & Bodenheimer, P. 2003, ApJ, 582, 869
Kobayashi, H., & Ida, S. 2001, Icar, 153, 416
Köhler, R., Petr-Gotzens, M. G., McCaughrean, M. J., et al. 2006, A&A, 458, 461
Kroupa, P. 2002, Sci, 295, 82
Kroupa, P. 2005, in ESA Special Publication 576, The Three-Dimensional Universe with Gaia, ed. C. Turon, K. S. O'Flaherty, & M. A. C. Perryman, (Noordwijk: ESA), 629
Kroupa, P., Aarseth, S., & Hurley, J. 2001, MNRAS, 321, 699
Lada, C. J., & Lada, E. A. 2003, ARA&A, 41, 57
Lada, C. J., Margulis, M., & Dearborn, D. 1984, ApJ, 285, 141
Leisawitz, D., Bash, F. N., & Thaddeus, P. 1989, ApJS, 70, 731
Li, G., & Adams, F. C. 2015, MNRAS, 448, 344
Lüghausen, F., Parmentier, G., Pflamm-Altenburg, J., & Kroupa, P. 2012, MNRAS, 423, 1985
Mamajek, E. E. 2009, in AIP Conf. Ser. 1158, Exoplanets and Disks: Their Formation and Diversity, ed. T. Usuda, M. Tamura, & M. Ishii, (Melville, NY: AIP), 3
Matsuyama, I., Johnstone, D., & Hartmann, L. 2003, ApJ, 582, 893
Matzner, C. D., & McKee, C. F. 2000, ApJ, 545, 364
McCaughrean, M. J., & O'dell, C. R. 1996, AJ, 111, 1977
Melioli, C., & de Gouveia dal Pino, E. M. 2006, A&A, 445, L23
Moeckel, N., Holland, C., Clarke, C. J., & Bonnell, I. A. 2012, MNRAS, 425, 450
Murray, N. 2011, ApJ, 729, 133
Olczak, C., Kaczmarek, T., Harfst, S., Pfalzner, S., & Portegies Zwart, S. 2012, ApJ, 756, 123
Olczak, C., Pfalzner, S., & Eckart, A. 2010, A&A, 509, A63
Olczak, C., Pfalzner, S., & Spurzem, R. 2006, ApJ, 642, 1140
Olczak, C., Spurzem, R., & Henning, T. 2011, A&A, 532, A119
Parker, R. J., Wright, N. J., Goodwin, S. P., & Meyer, M. R. 2014, MNRAS, 438, 620
Parmentier, G., & Baumgardt, H. 2012, MNRAS, 427, 1940
Pelupessy, F. I., & Portegies Zwart, S. 2012, MNRAS, 420, 1503
Pfalzner, S. 2004, ApJ, 602, 356
Pfalzner, S., & Kaczmarek, T. 2013a, A&A, 555, A135
Pfalzner, S., & Kaczmarek, T. 2013b, A&A, 559, A38
Pfalzner, S., & Olczak, C. 2007, A&A, 462, 193
Pfalzner, S., Olczak, C., & Eckart, A. 2006, A&A, 454, 811
Pfalzner, S., Parmentier, G., Steinhausen, M., Vincke, K., & Menten, K. 2014, ApJ, 794, 147
Pfalzner, S., Steinhausen, M., & Menten, K. 2014, ApJL, 793, L34
Pfalzner, S., Umbreit, S., & Henning, T. 2005a, ApJ, 629, 526
Pfalzner, S., Vincke, K., & Xiang, M. 2015b, A&A, 576, A28
Pfalzner, S., Vogel, P., Scharwächter, J., & Olczak, C. 2005c, A&A, 437, 967
Portegies Zwart, S. F. 2016, MNRAS, 457, 313
Portegies Zwart, S. F., McMillan, S. L. W., & Gieles, M. 2010, ARA&A, 48, 431
Rosotti, G. P., Dale, J. E., de Juan Ovelar, M., et al. 2014, MNRAS, 441, 2094
Scally, A., & Clarke, C. 2001, MNRAS, 325, 449
Scally, A., & Clarke, C. 2002, MNRAS, 334, 156
Shara, M. M., Hurley, J. R., & Mardling, R. A. 2016, ApJ, 816, 59
Shu, F. H., Adams, F. C., & Lizano, S. 1987, ARA&A, 25, 23
Spurzem, R. 1999, JCoAM, 109, 407
Steinhausen, M. 2013, PhD thesis, Mathematisch-Naturwissenschaftliche Fakultät der Universität zu Köln
Steinhausen, M., & Pfalzner, S. 2014, A&A, 565, A32
Störzer, H., & Hollenbach, D. 1999, ApJ, 515, 669
Vicente, S. M., & Alves, J. 2005, A&A, 441, 195
Vincke, K., Breslau, A., & Pfalzner, S. 2015, A&A, 577, A115
Vorobyov, E. I. 2011, ApJ, 729, 146
Xiang-Gruess, M. 2016, MNRAS, 455, 3086
Zwicky, F. 1953, PASP, 65, 205